


Article

# Fatigue Analysis of Printed Composites of Onyx and Kevlar

Moises Jimenez-Martinez <sup>1,\*</sup> , Julio Varela-Soriano <sup>1</sup>, Julio S. De La Trinidad-Rendon <sup>1</sup>, Sergio G. Torres-Cedillo <sup>2</sup>, Jacinto Cortés-Pérez <sup>2</sup> and Manuel Coca-Gonzalez <sup>1</sup>

<sup>1</sup> Tecnológico de Monterrey, School of Engineering and Science, 5718 Via Atlxycayotl, Puebla 72453, Mexico; j.varela@tec.mx (J.V.-S.); julio.delatrin@tec.mx (J.S.D.L.T.-R.); a01666072@tec.mx (M.C.-G.)

<sup>2</sup> Centro Tecnológico FES Aragón, Universidad Nacional Autónoma de México, Mexico City 57171, Mexico; sergiotorres98@aragon.unam.mx (S.G.T.-C.); jacop@unam.mx (J.C.-P.)

\* Correspondence: moisesjimenezmartinez@gmail.com

**Abstract:** The transformation of powertrains, powered by internal combustion engines, into electrical systems generates new challenges in developing lightweight materials because electric vehicles are typically heavy. It is therefore important to develop new vehicles and seek more aesthetic and environmentally friendly designs whilst integrating manufacturing processes that contribute to reducing the carbon footprint. At the same time, this research explores the development of new prototypes and custom components using printed composite materials. In this framework, it is essential to formulate new approaches to estimate fatigue life, specifically for components tailored and fabricated with these kinds of advanced materials. This study introduces a novel fatigue life prediction approach based on an artificial neural network. When presented with given inputs, this neural network is trained to predict the accumulation of fatigue damage and the temperature generated during cyclic loading, along with the mechanical properties of the compound. Its validation involves comparing the network's response with the load ratio result, which can be calculated using the fatigue damage parameter. Comparing both results, the network can successfully predict the fatigue damage accumulation; this implies an ability to directly employ data on the mechanical behavior of the component, eliminating the necessity for experimental testing. Then, the current study introduces a neural network designed to predict the accumulated fatigue damage in printed composite materials with an Onyx matrix and Kevlar reinforcement.

**Keywords:** composite; fatigue; additive manufacturing; damage; lightweight materials



**Citation:** Jimenez-Martinez, M.; Varela-Soriano, J.; De La Trinidad-Rendon, J.S.; Torres-Cedillo, S.G.; Cortés-Pérez, J.; Coca-Gonzalez, M. Fatigue Analysis of Printed Composites of Onyx and Kevlar. *J. Compos. Sci.* **2024**, *8*, 12. <https://doi.org/10.3390/jcs8010012>

Academic Editor: Kyong Yop Rhee

Received: 20 November 2023

Revised: 14 December 2023

Accepted: 28 December 2023

Published: 29 December 2023



**Copyright:** © 2023 by the authors. Licensee MDPI, Basel, Switzerland. This article is an open access article distributed under the terms and conditions of the Creative Commons Attribution (CC BY) license (<https://creativecommons.org/licenses/by/4.0/>).

## 1. Introduction

In the global economy, electromobility has become a central issue for automotive original equipment manufacturers and their suppliers. In addition, additive manufacturing (AM) is a key strategy for development time reduction, reducing or eliminating the tooling in other conventional processes in the future, such as foundry or stamping. Although AM components have been primarily used in prototyping, recent interest has been directed to their use as functional components in low production or customised components. This was because their structural strength and durability can increase their mobility applications, such as in automotive and aeronautical industries, generating lightweight structures [1,2].

However, these components must overcome mechanical and behavioural effects through manufacturing, which generates a thermal history. This history has detrimental effects on such components' mechanical properties, particularly in their long-term applications, as it causes damage due to dynamic and cyclic loads. All manufacturing processes inherently have variability in geometric tolerances, temporal changes and source material variations from different suppliers. However, in the case of AM, the main variables generate changes in the result (e.g., the cooling times and deposition speed of the material) when such materials transform from a semi-liquid process through the injector and form into a volumetric component. This variability poses a challenge for predicting the mechanical

behaviours in loads ranging from quasi-static to dynamic applications as transient or cyclic loads, similar to fatigue. This hinders the implementation of 3D-printed components in functional applications that must withstand cyclic loads without failure, cracks, stiffness or strength reduction in composites (matrix/reinforcement). Otherwise, these components will remain applied only in non-structural components [3,4].

Plastics, like metals, develop accumulated damage from repeated loads, which propagate until they reach a critical value along the surface or at an interface [5]. Although there are sometimes similarities between plastics and metal components, their damage processes are different. In metals, the damage nucleates and localises in a fissure that increases its length, propagating the crack until the catastrophic length develops failure. In composites, fatigue failure can be reached by mechanisms such as in heat generated by loads developing a stiffness reduction and matrix/fibre cracking debonding and delamination (interfacial failure) [6,7]. The fatigue process may be split into three main stages—nucleation, crack growth and failure—and the time for each stage depends on the materials and their constituents. In damage evaluation, the matrix, fibre or interface may be analysed considering the coupling element. In predicting component inter-phase failure, cohesive elements can be used to evaluate the softening that can generate relative displacement, delamination and fibre cracking, even under quasi-static loads [8,9]. This changes the mechanical behaviour of a material. This kind of change develops an accumulated process for cyclic loads, also known as fatigue failure. Thus, developing structural components printed with composites is important [10].

In a prior investigation of fatigue characterisation [11], an alternative approach using four-point bending was reported. This method incorporated a polymeric matrix composite material reinforced with embedded short fibre and continuous Kevlar fibre. The study employed numerical modelling and microscopy analysis to reveal the origin of failure modes. The numerical results were validated using experimental tests. Therefore, the computational model was validated using bulk mechanical properties instead of a complex model, which can require mechanical fatigue properties at each component of the composite material. One more study [12] reported that an ultrasonic fatigue test was conducted on a carbon-fibre-reinforced plastic material manufactured by 3D printing to assess its fatigue performance. In this study, we focused on specimens with two carbon fibre directions, including both unidirectional and BD (bidirectional) configurations. The designed specimen was extensively analysed across a range of low to high cycles during an ultrasonic fatigue test, and the differences in the lifespan of each specimen were accurately compared and validated. Another work, [13], examined the impact resistance of hybrid composites produced with material extrusion (MEX). The study involved applying impact energies of 20 J, 30 J, 40 J and 50 J to the specimens using the drop hammer impact test. The evidence presented in this work stated that the hybrids were proven to have robust impact resistance, exhibiting minimal damage and serving as effective high-energy absorbers.

Although the initial stress–strain behaviour of thermoplastics is linearly elastic, the non-linear development of viscoelasticity happens gradually with time. Printed composites generally reach a low elastic modulus, complicating their applications where displacement is a critical constraint [14–16]. Due to the viscoelastic characteristics of 3D-printed composite materials, the damage generated by cyclic loads must be predicted. This can be carried out using non-destructive techniques by monitoring the stiffness of a component and analysing its variation. It is important to consider the mechanical behaviour and physical response through temperature monitoring. In its nature, damage accumulation is an irreversible process that can be evaluated using a thermographic camera to monitor the heat generated by the internal friction of materials. This work deals with the accumulated damage prediction of fatigue in composites using neural networks in different frequency tests. Although the durabilities between 3 and 5 Hz were similar, the damage transitions were different. Using numerical techniques, such as neural networks, the fatigue life of composite materials printed in 3D can be predicted.

## 2. Damage in Composites

In structural components, the lifetime of the product must be predicted to guarantee that the operation is free of failure over time. At the beginning of component use, damage is not present and the concept of remaining life may be used. After transient, dynamic or quasi-static loads cause damage, the remaining life is partially consumed, and the damage is normalised between 0 and 1. When the damage reaches catastrophic failure, a value of 1 is attained, and there is no remaining life. This accumulated damage process is developed through dislocations, cavity slip bands, micro-crack nucleation, micro-propagation and macro-crack initiation and propagation until it reaches a specific length or modifies the component behaviour. To assess internal variables, measurements can be taken at macroscopic levels, including monitoring dynamic behaviour through techniques such as acoustic emissions or analysing the frequency response. Additionally, changes in mechanical response, such as stiffness behaviour, can be monitored.

Printed composite components can be considered a closed system, where the input mechanical energy  $w$  generated by loads is the result of the thermal energy  $\Delta Q$  modified by the internal energy  $\Delta U$  [10]. For viscoelastic materials, cyclic loads generate mechanical energy recovered for elastic behaviour. However, by its nature, some energy is transformed by damping characteristics (i.e., dissipated as thermal energy). This process changes the structural strength and generates an accumulated irreversible damage process expressed as a function of the mechanical energy:

$$W = \Delta U + \Delta Q \tag{1}$$

Using its thermal characteristics and considering that the only source of heat is generated by the loads, the effect of external heat is eliminated defining a reference, an internal heat source is not present before a crack and component behaviour using thermal evolution can be expressed as

$$\lambda \nabla^2 T = \rho c \dot{T} - \sigma^{ij} : \epsilon_{ij\text{plastic}} + A_i \dot{V}_i - T \left( \frac{\partial \sigma^{ij}}{\partial T} : \epsilon_{ij\text{elastic}} + \frac{\partial A_i}{\partial T} V_i \right) \tag{2}$$

where  $\lambda$  is the thermal conductivity,  $T$  is the maximum temperature,  $c$  is the specific heat,  $\sigma^{ij}$  is the stress tensor and  $\epsilon_{ij\text{elastic}}$  and  $\epsilon_{ij\text{plastic}}$  are the elastic and plastic strain tensors;  $V_i$  stands for the internal variables related to the FDM printed component (Liakat).

During cyclic loads, the printed component dissipates heat via conduction. This dissipation is greater through all the components than the heat concentration on the fissure. Under this assumption, the term  $\lambda \nabla^2 T$  can be neglected and the elastic tensor can be roughly approximated to zero. The equivalent damage by the stress in the plastic strain is related to the temperature as follows:

$$\rho c \dot{T} = \sigma^{ij} : \epsilon_{ij\text{plastic}} + A_i \dot{V}_i + \frac{\partial A_i}{\partial T} V_i T \tag{3}$$

When constant material characteristics are considered, the damage process of the stiffness degradation with the temperature can be analysed [17,18].

The main aspects that detrimentally affect the fatigue strength and residual life can be summarised as loads, design, material (matrix and reinforcement) and manufacturing. The reinforcement structure, lay-up sequence, residual stress due to the manufacturing process, stress ratios and frequency and waveform of the cyclic loading affect fatigue strength. Figure 1 shows the interrelation between the main parameters that influence the accumulated damage generated by fatigue.

Although the parameters that contribute to fatigue strength in composites are similar to those in metals a priori, their performance and monitoring exhibit changes. Cyclic loading involves the transition process of traction plus compression, depending on maximum- and minimum-amplitude ratios. The failure of composites under compression involves different mechanisms, and these show a lower strength compared with those under tensile

loading. Ideally, the aim is to strengthen the matrix of a component with fibres that behave as a single material; however, the stiffness ratio may result in the separation of certain types of loads, such as compression.

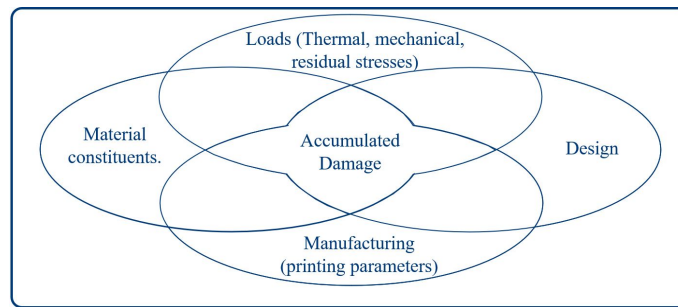


**Figure 1.** Parameters in fatigue strength in printed composites.

The most common failure mode for stiff fibres embedded in a compliant matrix is known as micro-buckling. It can occur along two competing modes: without a phase shift (Figure 2b) or without a phase shift (Figure 2c). It could generate a fibre fracture as an isolated material but with debonding and general failure at a composite level [19].

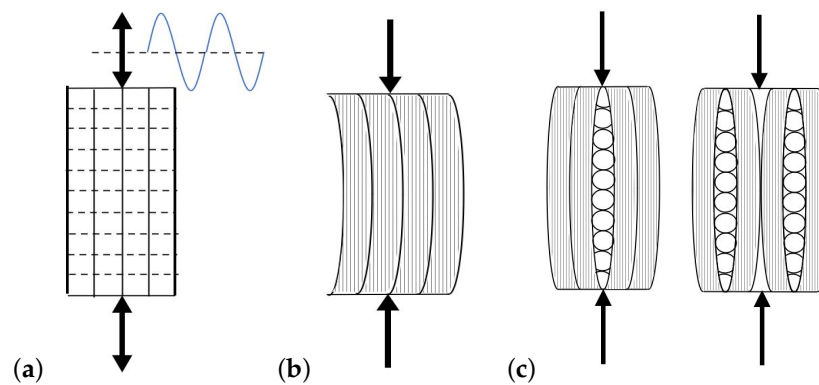


**Figure 2.** Schematic behaviour of cyclic loads in printed composites: (a) composites under cyclic load, (b) compression with matrix and reinforcement in phase and (c) schematic types of debonding of layers.

The cyclic loads applied to a structural component depend on a load history, which is generated by its operating conditions. Inherently, some levels of dispersion exist because of factors like the sequence of loads, variations as a function of the mean load value and fluctuations within the load itself due to the relationship between the minimum and maximum value of the cycle ( $R$ ), as seen in Figure 3.

Damage in composites is non-linear. Although it is evaluated based on the response of the matrix and reinforcement, mechanical strength decreases under loads in three stages, as shown in Figure 4. These materials are sensitive to damage, and their structural strength can be analysed through static, fatigue, creep analyses and the relationship among these failures. Static mechanical responses can be used as input information for the dynamic processes of damage accumulation [20].

Fibre-reinforced composites have been widely used in aerospace, marine, automotive and advanced engineering applications in recent years because of their high-quality mechanical properties. However, these structures always suffer from cyclic loading during their service life. The damage propagation in these structures is accumulated in a damage process, as in other materials. However, the main difference lies in two main response materials: from the matrix and from reinforcement. As a unit, these composites have a general strength that is reduced (Figure 5).

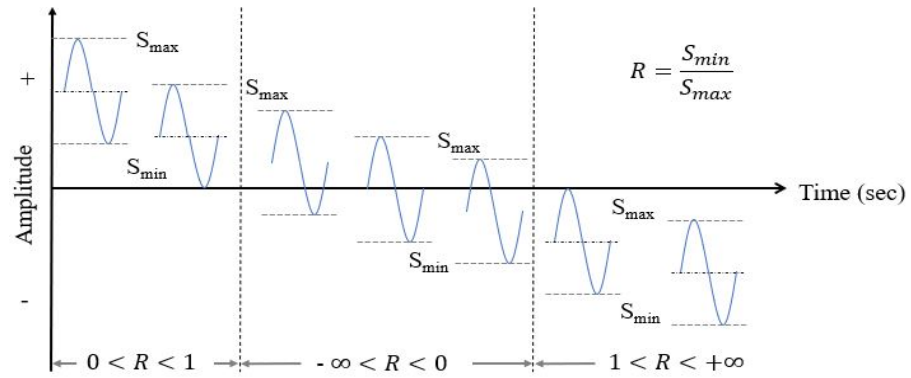


**Figure 3.** Schematic definition of the ratio between the minimum and maximum amplitude in a cyclic load.

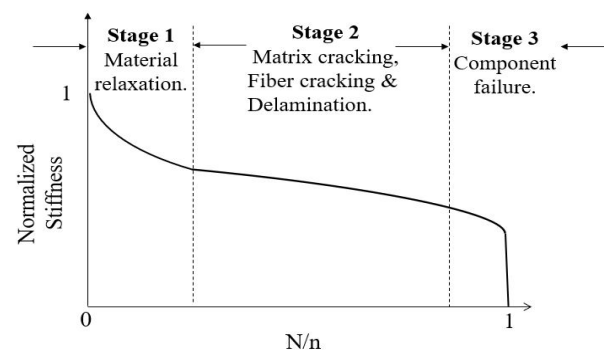


**Figure 4.** Damage evolution process in printed composites.

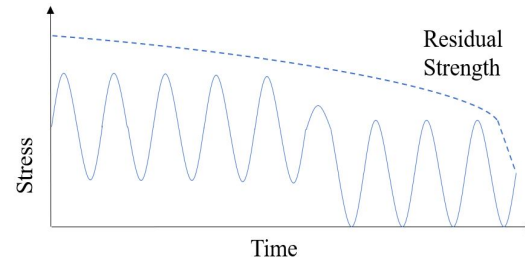


**Figure 5.** Mechanical strength reduction as a function of dynamic loads.

The composite strength is reduced by obtaining a response with a lower stiffness  $k$  which is related to the material properties through the Young modulus. Its value can be used as a measure of damage using  $k_0$  at failure  $k_f$  and  $k_n$  at  $n_{th}$  cycles. The fatigue damage parameter  $D_N$  can be defined as

$$D_N = \frac{k_0 - k_n}{k_0 - k_f} \tag{4}$$

The stiffness can be measured by performing measurements during the test at different intervals [21,22] or a priori during the operation. Ref. [23] proposed a real-time composite prediction method combining Bayesian inference and sensors. This method involves using measurements as parameters in a closed-loop system to obtain the load and corresponding displacement data under the same measurement conditions.

The degradation of fibre direction strength during fatigue cycling is assumed to follow a simple linear degradation per cycle. The residual strength  $R_{II}^r$  in the fibre direction is expressed by

$$R_{II}^r = R_u^s - \sum_{i=1}^m (R_{II}^s - \sigma_m) \frac{N_i}{N_f \sigma_m} \tag{5}$$

where  $m$  is the number of fatigue cyclic blocks,  $N_i$  is the number of fatigue cycles,  $R_u^s$  is the static fibre direction strength and  $N_i$  is the number of cycles to failure in constant amplitude at  $\sigma_m$ . However, evaluating the printed component as a unit, the stiffness degradation is evaluated considering the matrix and fibre overall response [24].

### 3. Damage Analysis Using an Artificial Neural Network

An artificial neural network (ANN) is an adaptive process used to simulate relationships between the source of information (input) and the expected behaviour (output) by adjusting these relationships through different weights ( $w$ ). The selection of inputs depends on the phenomenological process analysed; sometimes, the chemical composition may be used to get the mechanical responses as output [25]. In other analyses, mechanical responses are used as inputs, with the addition of synthetic responses for improving the development of relationships and predict fatigue life.

The printing process and the filament used have an impact on the mechanical behaviour and durability [26,27]. However, despite considerable advancements in AM techniques, 3D-printed parts still face issues related to fatigue life according to the thermal process generated during their processing. Thus, non-linear analysis can be used to reduce the time and development cost in AM to improve the overall mechanical strength of materials [28,29].

Thus, ANN has been proposed for predicting fatigue life. The backpropagation algorithm adjusts the weights in a supervised training process. For this process, the data employed are divided into training, validation and testing data. All the inputs are fed to the neuron. The phenomenon analysed is related to an expected output based on different weights  $w_i$  to connect two neurons along the network at different  $k_{th}$  layers, expressed by

$$net_{i,k} = \left[ \sum_j w_{i,j,k} out_{j,k-1} \right] + \theta_{i,k} \tag{6}$$

where  $w_{i,j,k}$  is the weight for node  $j$  in the  $(k - 1)_{th}$  layer to node  $i$ . The interconnected weights are iteratively updated until the mean square error is reduced and is inside a threshold value. The process is updated by

$$w_{ji}(t + 1) = \alpha w_{ji}(t) + \eta x_i f'(net_j^k) \sum_{i=1}^N (d_i - z_i) f'(net_j^O) w_{ij} \tag{7}$$

where  $d_i$  is the desired response,  $z_i$  is the actual response,  $\eta$  is the learning rate,  $t$  is the iterative sample,  $x_i$  is the input pattern and  $net_j^O$  is the input to the connection at node  $j$  located at the  $t_{th}$  layer.

The inputs are connected using a hidden layer, and the topology of the proposed ANN is shown in Figure 6. Therein, the inputs  $x$  are the load amplitude, mechanical properties such as normalised stiffness and its components (force and displacement) and the temperature at different cycles; the damage evolution and the desired output are the cycle results of the experimental tests.

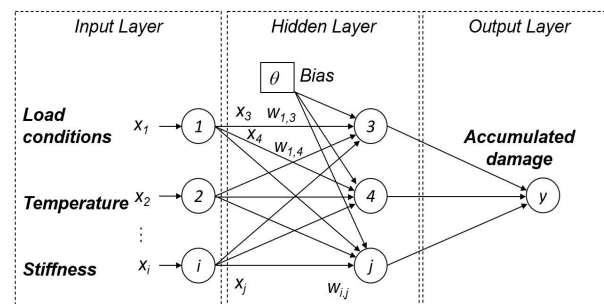


Figure 6. Multilayer neural network.



#### 4. Additive Manufacturing

All specimens in this study were printed using the same Markforged printer, using an Onyx (2.4 GPa tensile modulus and 1.2 g/cm<sup>3</sup> density) as a matrix and Kevlar (27 GPa tensile modulus and 1.2 g/cm<sup>3</sup> density) as a reinforcement with a configuration of 0°, 45°, 90° and 135°. The layer height was 0.1 mm. Figure 7 shows the schematic printing process with temperatures of 275 °C and 145 °C for Onyx and Kevlar, and every filament had its own nozzle.

The percentages of fibre (onyx) and reinforcement (kevlar) depend on the reinforcement layers. In the case of three layers of reinforcement, this configuration is 78% matrix and 22% fibre. In another case of two-layer reinforcement components, the composition is 84% matrix and 16% reinforcement. In one-layer reinforcement configuration, there is 94% matrix and 6% kevlar reinforcement, respectively.

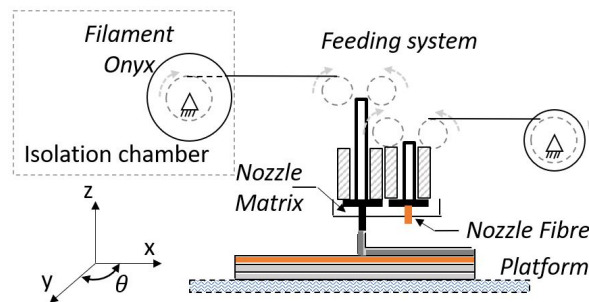


Figure 7. Schematic printing process.

#### 5. Experimental Tests

##### 5.1. Quasistatic Tests

The effect of maximum- and minimum-load ratios on the fatigue life of composite materials has been reported. Herein, tests were performed on components only with the matrix (Onyx), matrix plus one reinforcement layer (Onyx + 1C), matrix and two layers (Onyx + 2C) and matrix and three reinforcement layers (Onyx + 3C) in order to understand the effect of tensile and compressive loads. An expected behaviour is a different response between the traction and compression. The tensile and compression tests were performed in an Instron universal machine. Figure 8 shows the compression test.

Then, the true stress and strain are computed using the following equations:

$$\sigma_t = \frac{P}{A} e^{\epsilon_t} \tag{8}$$

$$\epsilon_t = \ln(1 + \delta) \tag{9}$$

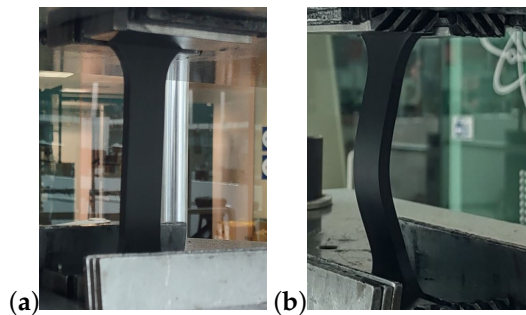
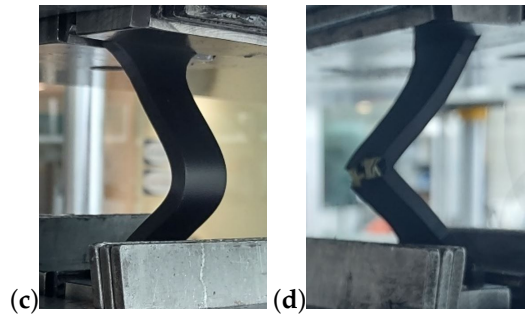
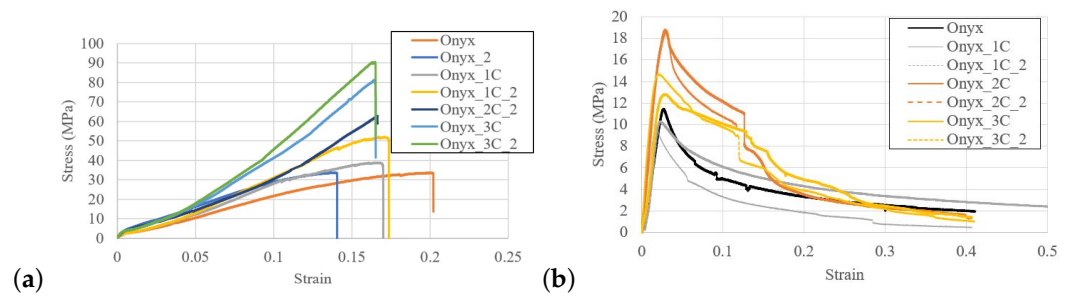


Figure 8. Cont.



**Figure 8.** Compression test. (a) Printed component in test machine (b), response with onyx, (c), behaviour with reinforcement of Kevlar and (d) final failure.

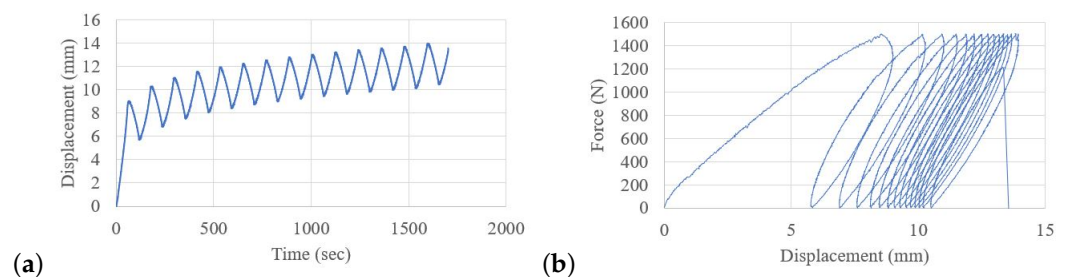
The reinforcement behaviour can be observed for the strain-to-tensile curve response (Figure 9a). Because constant zones were observed for each reinforcement when only the Onyx matrix was used, the response was of a conventional material. However, with compression (Figure 9b), the decay after the maximum value was obtained, and only an abrupt change in the rupture of one of the fibres was observed.



**Figure 9.** Stress-strain curves: (a) tensile and (b) compression.

5.2. Transient Response

The creep curve represents the elastic instantaneous response, which is etarded elastic deformation due to the viscous behaviour. Although this is partially reversible, it takes time to conduct. Figure 10a shows the response of the matrix when the cyclic load is applied. As shown in Figure 10b, the displacement was increased until failure. Interestingly, a significant interaction of stiffness and displacement evolution was also observed.



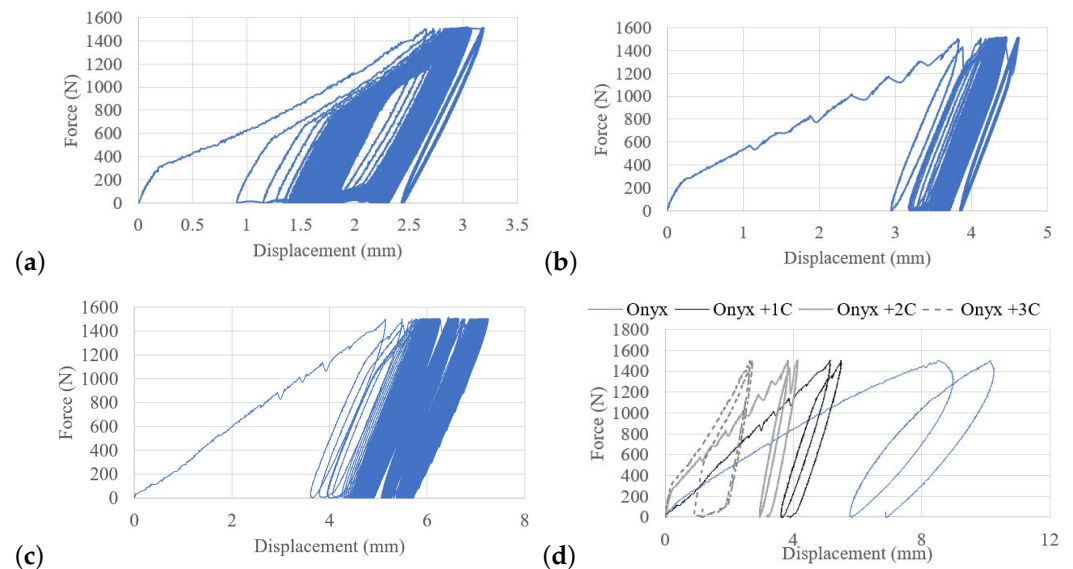
**Figure 10.** Stiffness measurement at a cyclic load of 0–1500 N: (a) displacement response vs. time and (b) dynamic stiffness.

Figure 10b shows how damage is accumulated based on the dynamic stiffness. Figure 10a shows the evolution of the damage based on what is required for more displacement to reach the constant load.

Figure 11 shows the behavior of printed components with reinforcement. Figure 11a–c show the response of applying the load of 0–1500 N, suspending the test at 24 h without failure (run out). Figure 11d shows an approximation of the first two cycles, where the



first plastic deformation is observed. For components with reinforcement, a more linear discharge zone is observed; however, at the end of it, a non-linear recovery is observed, which depends on the number of reinforcement layers.



**Figure 11.** Dynamic stiffness at cyclic load of 0–1500 N: (a) three reinforcement layers, (b) two reinforcement layers, (c) one reinforcement layer and (d) comparison of the first two cycles of onyx with and without reinforcement.

### 5.3. Fatigue Tests

A uniaxial fatigue test machine was used to evaluate the cyclic response (Figure 12). A load of 2000 N was applied using a relationship of  $R = -1$ , and tests were performed at 2, 3, 4 and 5 Hz.

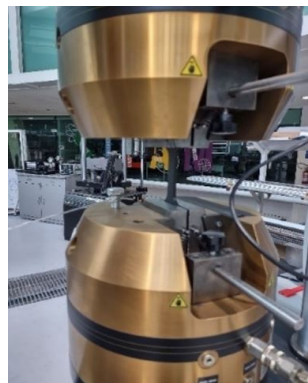


**Figure 12.** Test set-up for fatigue assessment.

Turning now to experimental evidence, measurements of the mechanical behaviour as force vs. displacement were performed considering the thermal history (Figure 13). The evolution of the temperature has a direct relation with the accumulated damage. Figure 13a shows the generalised temperature throughout the component. After the first stage of the damage, the increase tended to be located at the expected failure zone (Figure 13b). This temperature was then localised at critical points (Figure 13c) until the final failure (Figure 13d).

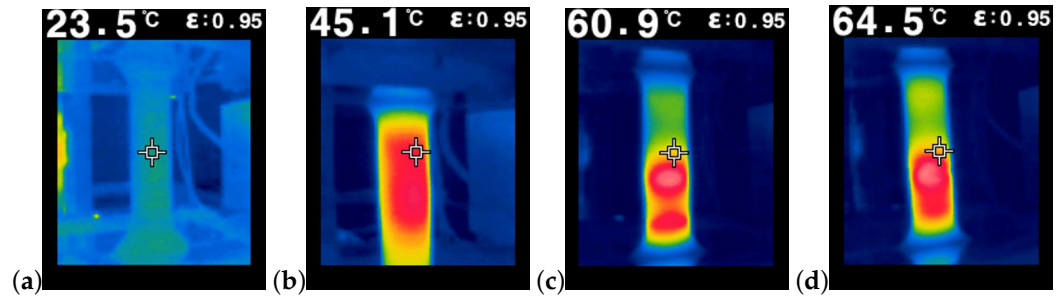


Figure 13. Temperature evolution until failure.

The stiffness was evaluated regarding the history of evolution as a function of temperature. At high temperatures, the scatter of stiffness increased at all frequencies (Figure 14). Figure 14a, 14b, 14c and 14d show the sampling performed during the tests at 2 Hz, 3 Hz, 4 Hz and 5 Hz, respectively.

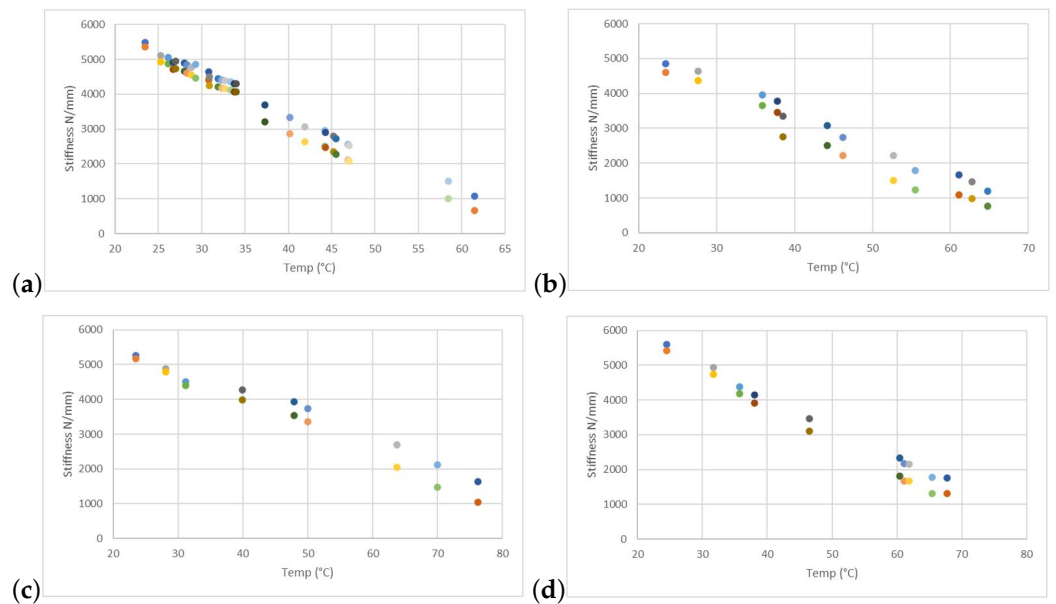


Figure 14. Stiffness evolution as a function of temperature at different frequencies. (a) 2 Hz, (b) 3 Hz, (c) 4 Hz and (d) 5 Hz.

### 6. Results and Discussion

Predicting the accumulated damage behaviour of advanced materials under cyclic loads is important to predict their fatigue life. By knowing the accumulated damage and the residual life, printed components of composite materials can be developed for structural and functional use. To this end, processes that consider non-linear processes must be developed. Figure 15 shows different failures. Figure 15a shows matrix cracking, Figure 15b shows matrix/fibre cracking, Figure 15c shows matrix/fibre debonding and Figure 15d shows the complete failure.

Figure 16 presents the failure mechanism. Figure 16a illustrates the areas of brittle failure in the contour of the component and ductility within the part near the reinforcing fibre. Figure 16b shows that there is no reduction zone in the area of the filament of the printed matrix, showing brittle behaviour. In Figure 16c, it is shown that the filaments have a reduced area in the failure area, showing ductile failure. It is believed that the space between the printed filaments generates a stress concentrator.

The change in stiffness over the useful life of the component was analysed to know the effect of the load frequency on damage evolution, as shown in Figure 17. The damage transition zones were different. At 2 Hz of load (Figure 17a), a smooth transition zone

was observed in the first and second stages of the residual damage. However, an abrupt change was observed between the second and third stages. Meanwhile, at 5 Hz, a smooth transition zone was observed in both zones. The final failure propagation was very fast, as shown in Figure 17d. Although the duration was similar at load frequencies of 3, 4 and 5 Hz, the behaviour was not.

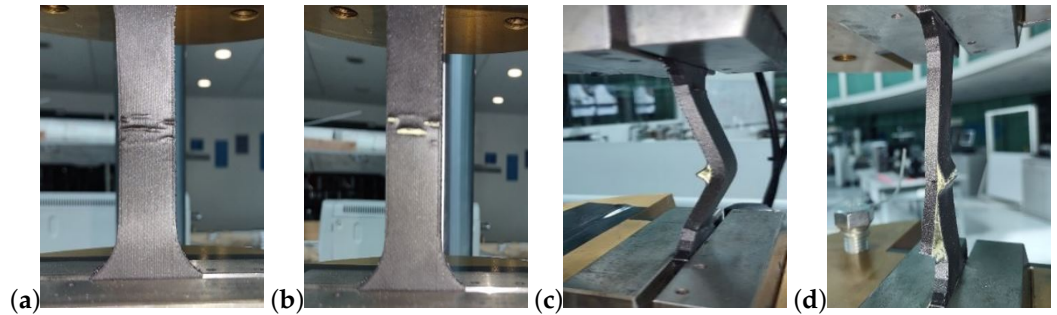


**Figure 15.** Damage during tests: (a) internal cracking, (b) matrix/fibre failure, (c) matrix/fibre debonding and (d) final failure.

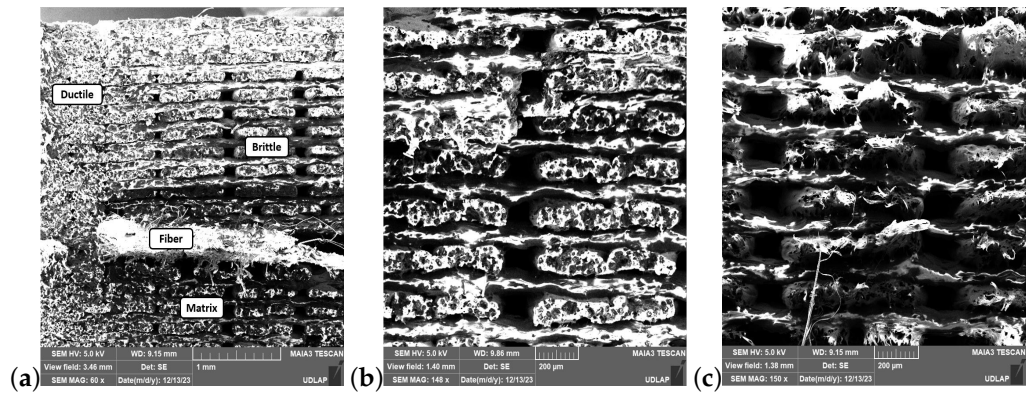


**Figure 16.** SEM analysis: (a) comparison between ductile and brittle failure, (b) brittle behaviour and (c) ductile behaviour.

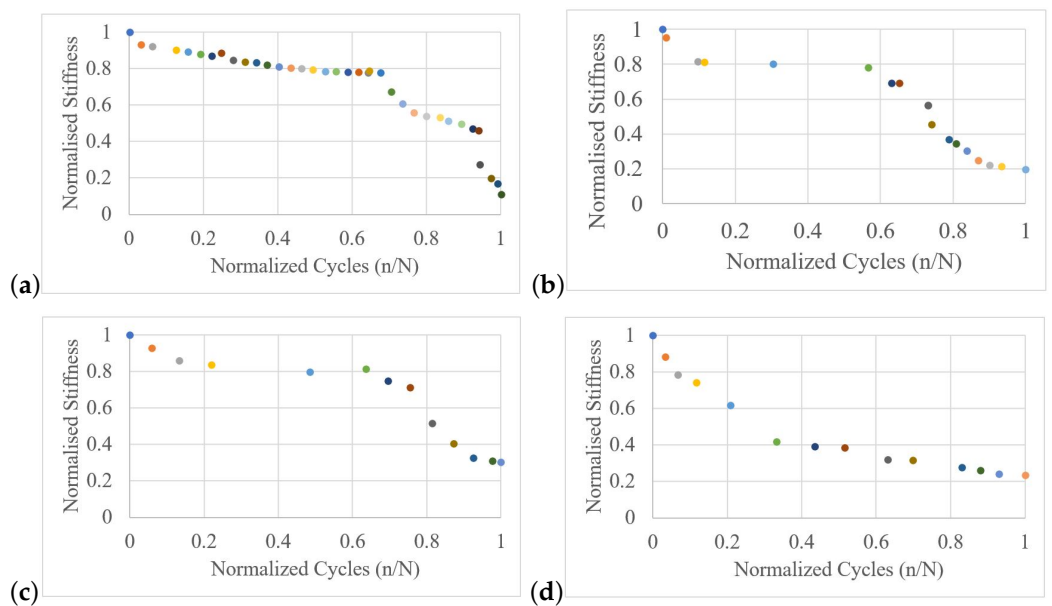


**Figure 17.** Normalised stiffness vs. normalised cycles: (a) 2Hz, (b) 3Hz, (c) 4 Hz and (d) 5 Hz.

Figure 18 compares the damage evolution at different frequencies, comparing the prediction with neural networks. The need to conduct life prediction using non-linear methods is evident because of the materials' inherent non-linear behaviour. Thus, methods that update the behaviour of mechanical responses during evaluation must be developed.

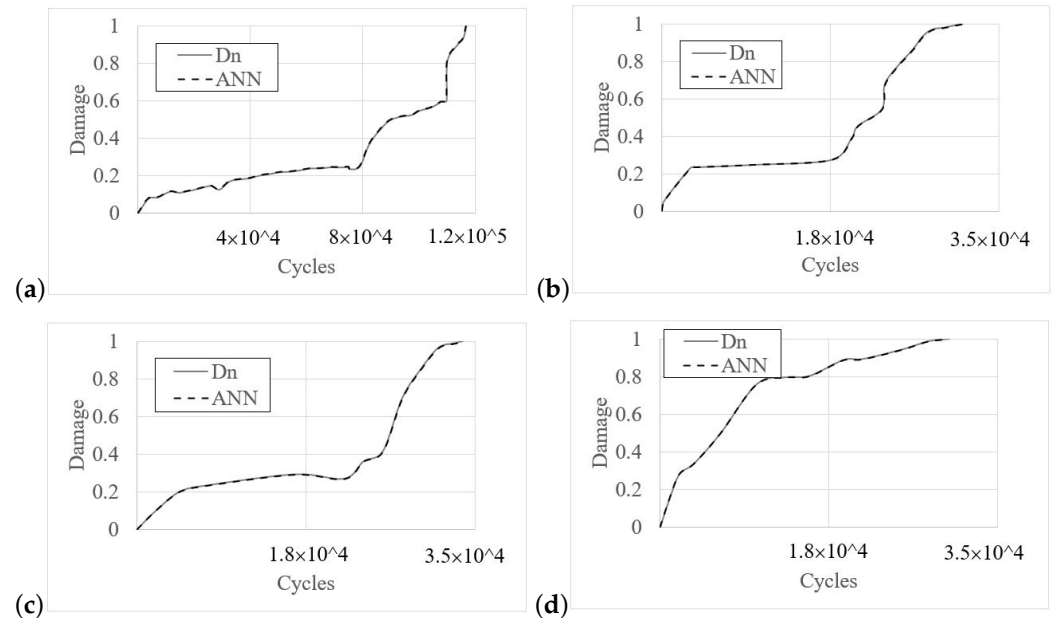


**Figure 18.** Damage prediction with neural network: (a) 2 Hz, (b) 3 Hz, (c) 4 Hz and (d) 5 Hz.

For metal alloys, approximately 80–90% of the total fatigue life is required for crack initiation, whereas approximately 10–20% is required for crack growth. Once a crack is initiated, the crack grows relatively fast. For composites, approximately 10–20% (or less) of the fatigue life is related to crack initiation, 75–85% is related to crack growth and approximately 5% of the damage is related to rapid catastrophic failure. The last rapid growth can be seen at the load frequencies of 2, 3 and 4 Hz (Figure 17a–c). However, only a smooth transition can be seen at 5 Hz.

The overall behaviour of the damage was determined using the responses shown in Figures 14, 17 and 18. When the stiffness has a linear (flat) response, as in Figure 13, the temperature rises. After the heat accumulates and finally increases, the stiffness drops. These results suggest an association between the load velocity and the transitions between the residual life stages.

For monitoring damage evolution, the initial and final stiffness of  $5000 \pm 500$  N and  $1300 \pm 500$  N were used. The failure temperature was  $65 \text{ }^\circ\text{C} \pm 2 \text{ }^\circ\text{C}$ , except for the test frequency of 4 Hz, where a temperature of  $76 \text{ }^\circ\text{C}$  was reached to achieve the final stiffness. The ratio between the minimum and maximum loads of the load was  $R = -1$ . The amplitude of the maximum cycle, based on the compressive force, should be defined. The maximum compressive force was one-fifth of the compressive force when we had three reinforcement sections. In all cases, a reduction in the compressive stress was observed. However, when only Onyx was used, the maximum strength was one-third of the tensile stress, as shown in Figure 10. In accordance with the present results, previous studies have demonstrated that the filament alignment results in a structural response related to the load case, where the tensile behaviour depends on the filament orientation relative to the loading direction, as described by the authors of [4].

Although three stages of damage were expected, using Figures 17a and 18a, we can define four areas at 2 Hz. The recovery of the response generated practically linear behaviour, i.e., there was no abrupt change or constant reduction between 0.25% and 0.65% of the normalised cycles. Material parameters were used to improve fatigue life prediction,

resulting in the use of additional tests. One of the advantages of neural networks is the direct use of data from mechanical behaviour, eliminating the need for experimental testing.

## 7. Conclusions

We analysed the damage accumulation process in composite printed parts of Onyx with a reinforcement of Kevlar. The findings of this research provide insights into fatigue life prediction using neural networks.

- Fatigue life prediction in thermoplastics is complex as they initially behave linearly, but this behaviour changes to their non-linear response over time due to their viscoelastic response.
- The damage accumulated by fatigue in composite materials can be predicted using the result of the load ratio, which can be expressed using the stiffness obtained by the maximum and minimum loads applied to the component.
- Neural networks were used to predict the fatigue life of components manufactured using AM with an Onyx matrix and reinforced with Kevlar, considering a constant amplitude load. The predictions using ANNs had errors of 0.0015%, 0.083%, 0.02% and 0.012% at 2, 3, 4 and 5 Hz, respectively.

Notwithstanding the relatively limited sample, this work offers valuable insights into the analysis of the fatigue life of composite printed components. The generalisability of these results is subject to certain limitations. For instance, it cannot be extrapolated to other conditions.

**Author Contributions:** Conceptualisation, M.J.-M. and J.V.-S.; methodology, M.J.-M.; validation, J.S.D.L.T.-R., M.C.-G., S.G.T.-C., J.C.-P. and M.J.-M.; formal analysis, J.S.D.L.T.-R., M.C.-G. and M.J.-M.; investigation, J.V.-S. and M.J.-M.; resources, M.J.-M.; data curation, J.S.D.L.T.-R., S.G.T.-C., J.C.-P. and M.J.-M.; writing—original draft preparation, S.G.T.-C. and M.J.-M.; writing—review and editing, M.J.-M.; visualisation, J.S.D.L.T.-R., M.C.-G., S.G.T.-C., J.C.-P. and M.J.-M.; supervision, M.J.-M. All authors have read and agreed to the published version of the manuscript.

**Funding:** This research received no external funding.

**Data Availability Statement:** The data presented in this study are available on request from the corresponding author.

**Acknowledgments:** The authors are grateful for the support of the Carrera of the Department of Mechanics of UDLAP for his support in the Scanning Electron Microscopy (SEM) analysis.

**Conflicts of Interest:** The authors declare no conflicts of interest.

## References

1. Hegab, H.; Khanna, N.; Monib, N.; Salem, A. Design for sustainable additive manufacturing: A review. *Sustain. Mater. Technol.* **2023**, *35*, e00576. [\[CrossRef\]](#)
2. Kanishka, K.; Acherjee, B. A systematic review of additive manufacturing-based remanufacturing techniques for component repair and restoration. *J. Manuf. Process.* **2023**, *89*, 220–283. [\[CrossRef\]](#)
3. Ford, S.; Minshall, T. Invited review article: Where and how 3D printing is used in teaching and education. *Addit. Manuf.* **2019**, *25*, 131–150. [\[CrossRef\]](#)
4. Lampron, O.; Lingua, A.; Therriault, D.; Lévesque, M. Characterization of the non-isotropic tensile and fracture behavior of unidirectional polylactic acid parts manufactured by material extrusion. *Addit. Manuf.* **2023**, *61*, 103369. [\[CrossRef\]](#)
5. Abbasi, S.; Ladani, R.; Wang, C.; Mouritz, A. Improving the delamination fatigue resistance of composites by 3D woven metal and composite Z-filaments. *Compos. Part A Appl. Sci. Manuf.* **2021**, *147*, 106440. [\[CrossRef\]](#)
6. Safai, L.; Cuellar, J.S.; Smit, G.; Zadpoor, A.A. A review of the fatigue behavior of 3D printed polymers. *Addit. Manuf.* **2019**, *28*, 87–97. [\[CrossRef\]](#)
7. Shiri, S.; Yazdani, M.; Pourgol-Mohammad, M. A fatigue damage accumulation model based on stiffness degradation of composite materials. *Mater. Des.* **2015**, *88*, 1290–1295. [\[CrossRef\]](#)
8. Tao, C.; Mukhopadhyay, S.; Zhang, B.; Kawashita, L.F.; Qiu, J.; Hallett, S.R. An improved delamination fatigue cohesive interface model for complex three-dimensional multi-interface cases. *Compos. Part A Appl. Sci. Manuf.* **2018**, *107*, 633–646. [\[CrossRef\]](#)
9. Dhar, M.; Das, A.; Shome, A.; Borbora, A.; Manna, U. Design of ‘tolerant and hard’ superhydrophobic coatings to freeze physical deformation. *Mater. Horiz.* **2021**, *8*, 2717–2725. [\[CrossRef\]](#)



10. Movahedi-Rad, A.V.; Eslami, G.; Keller, T. A novel fatigue life prediction methodology based on energy dissipation in viscoelastic materials. *Int. J. Fatigue* **2021**, *152*, 106457. [[CrossRef](#)]
11. Pertuz-Comas, A.D.; Díaz, J.G.; Meneses-Duran, O.J.; Niño-Álvarez, N.Y.; León-Becerra, J. Flexural Fatigue in a Polymer Matrix Composite Material Reinforced with Continuous Kevlar Fibers Fabricated by Additive Manufacturing. *Polymers* **2022**, *14*, 3586. [[CrossRef](#)] [[PubMed](#)]
12. ho Jung, C.; Kang, Y.; Song, H.; Lee, M.G.; Jeon, Y. Ultrasonic fatigue analysis of 3D-printed carbon fiber reinforced plastic. *Heliyon* **2022**, *8*, e11671. [[CrossRef](#)] [[PubMed](#)]
13. Akmal Zia, A.; Tian, X.; Jawad Ahmad, M.; Tao, Z.; Meng, L.; Zhou, J.; Zhang, D.; Zhang, W.; Qi, J.; Li, D. Impact Resistance of 3D-Printed Continuous Hybrid Fiber-Reinforced Composites. *Polymers* **2023**, *15*, 4209. [[CrossRef](#)] [[PubMed](#)]
14. Foroughi, A.H.; Valeri, C.; Jiang, D.; Ning, F.; Razavi, M.; Razavi, M.J. Understanding compressive viscoelastic properties of additively manufactured PLA for bone-mimetic scaffold design. *Med. Eng. Phys.* **2023**, *114*, 103972. [[CrossRef](#)] [[PubMed](#)]
15. Markandan, K.; Lai, C.Q. Fabrication, properties and applications of polymer composites additively manufactured with filler alignment control: A review. *Compos. Part B Eng.* **2023**, *256*, 110661. [[CrossRef](#)]
16. Mayén, J.; Del Carmen Gallegos-Melgar, A.; Pereyra, I.; Poblano-Salas, C.A.; Hernández-Hernández, M.; Betancourt-Cantera, J.; Mercado-Lemus, V.; Del Angel Monroy, M. Descriptive and inferential study of hardness, fatigue life, and crack propagation on PLA 3D-printed parts. *Mater. Today Commun.* **2022**, *32*, 103948. [[CrossRef](#)]
17. Skinner, T.; Datta, S.; Chattopadhyay, A.; Hall, A. Fatigue damage behavior in carbon fiber polymer composites under biaxial loading. *Compos. Part B Eng.* **2019**, *174*, 106942. [[CrossRef](#)]
18. Jia, Z.; Pastor, M.L.; Garnier, C.; Gong, X. Fatigue life determination based on infrared thermographic data for MultiDirectional (MD) CFRP composite laminates. *Compos. Struct.* **2023**, *319*, 117202. [[CrossRef](#)]
19. Safdar, N.; Daum, B.; Rolfes, R. The effect of model dimensionality on compression strength of fiber reinforced composites. *J. Compos. Mater.* **2022**, *56*, 4645–4662. [[CrossRef](#)]
20. Zhang, X.; Hoa, S.V.; Li, Y.; Xiao, J.; Tan, Y. Effect of Z-pinning on fatigue crack propagation in composite skin/stiffener structures. *J. Compos. Mater.* **2018**, *52*, 275–285. [[CrossRef](#)]
21. Suzuki, T.; Mahfuz, H.; Takanashi, M. A new stiffness degradation model for fatigue life prediction of GFRPs under random loading. *Int. J. Fatigue* **2019**, *119*, 220–228. [[CrossRef](#)]
22. Ziemian, C.; Ziemian, R.; Haile, K. Characterization of stiffness degradation caused by fatigue damage of additive manufactured parts. *Mater. Des.* **2016**, *109*, 209–218. [[CrossRef](#)]
23. Peng, T.; Liu, Y.; Saxena, A.; Goebel, K. In-situ fatigue life prognosis for composite laminates based on stiffness degradation. *Compos. Struct.* **2015**, *132*, 155–165. [[CrossRef](#)]
24. Zhao, Y.; Chen, Y.; Zhou, Y. Novel mechanical models of tensile strength and elastic property of FDM AM PLA materials: Experimental and theoretical analyses. *Mater. Des.* **2019**, *181*, 108089. [[CrossRef](#)]
25. Jiménez-Armendáriz, J.; Jimenez-Martinez, M.; Varela-Soriano, J.; Santana Diaz, A.; Perez Santiago, R. Energy Dissipation Enhancement of Thin-Walled 6063 T5 Aluminium Tubes by Combining a Triggering Mechanism and Heat Treatment. *Metals* **2023**, *13*, 922. [[CrossRef](#)]
26. Shanmugam, V.; Das, O.; Babu, K.; Marimuthu, U.; Veerasimman, A.; Johnson, D.J.; Neisiany, R.E.; Hedenqvist, M.S.; Ramakrishna, S.; Berto, F. Fatigue behaviour of FDM-3D printed polymers, polymeric composites and architected cellular materials. *Int. J. Fatigue* **2021**, *143*, 106007. [[CrossRef](#)]
27. Azadi, M.; Dadashi, A.; Dezianian, S.; Kianifar, M.; Torkaman, S.; Chiyani, M. High-cycle bending fatigue properties of additive-manufactured ABS and PLA polymers fabricated by fused deposition modeling 3D-printing. *Forces Mech.* **2021**, *3*, 100016. [[CrossRef](#)]
28. Parsazadeh, M.; Sharma, S.; Dahotre, N. Towards the next generation of machine learning models in additive manufacturing: A review of process dependent material evolution. *Prog. Mater. Sci.* **2023**, *135*, 101102. [[CrossRef](#)]
29. Zhan, Z.; Li, H. A novel approach based on the elastoplastic fatigue damage and machine learning models for life prediction of aerospace alloy parts fabricated by additive manufacturing. *Int. J. Fatigue* **2021**, *145*, 106089. [[CrossRef](#)]

**Disclaimer/Publisher's Note:** The statements, opinions and data contained in all publications are solely those of the individual author(s) and contributor(s) and not of MDPI and/or the editor(s). MDPI and/or the editor(s) disclaim responsibility for any injury to people or property resulting from any ideas, methods, instructions or products referred to in the content.